Progress in PHOTOVOLTAICS

PROGRESS IN PHOTOVOLTAICS: RESEARCH AND APPLICATIONS
Prog. Photovolt: Res. Appl. (2016)
Published online in Wiley Online Library (wileyonlinelibrary.com). DOI: 10.1002/pip.2764

SHORT COMMUNICATION

Electronic structure of the Zn(O,S)/Cu(In,Ga)Se_2 thin-film solar cell interface

Michelle Mezher[1]*, Rebekah Garris[2], Lorelle M. Mansfield[2], Kimberly Horsley[1], Lothar Weinhardt[1,3,4,5], Douglas A. Duncan[1], Monika Blum[1], Samantha G. Rosenberg[1], Marcus Bär[1,6,7], Kannan Ramanathan[2] and Clemens Heske[1,3,4,5]*

[1] Department of Chemistry and Biochemistry, University of Nevada, Las Vegas (UNLV), Las Vegas, NV 89154 USA
[2] National Renewable Energy Laboratory (NREL), Golden, CO 80401, USA
[3] Institute for Photon Science and Synchrotron Radiation (IPS), Karlsruhe Institute of Technology (KIT), 76344 Eggenstein-Leopoldshafen, Germany
[4] ANKA Synchrotron Radiation Facility, Karlsruhe Institute of Technology (KIT), 76344 Eggenstein-Leopoldshafen, Germany
[5] Institute for Chemical Technology and Polymer Chemistry (ITCP), Karlsruhe Institute of Technology (KIT), 76128 Karlsruhe, Germany
[6] Renewable Energy, Helmholtz-Zentrum Berlin für Materialien und Energie GmbH, 14109 Berlin, Germany
[7] Institut für Physik und Chemie, Brandenburgische Technische Universität Cottbus-Senftenberg, 03046 Cottbus, Germany

ABSTRACT

The electronic band alignment of the Zn(O,S)/Cu(In,Ga)Se_2 interface in high-efficiency thin-film solar cells was derived using X-ray photoelectron spectroscopy, ultra-violet photoelectron spectroscopy, and inverse photoemission spectroscopy. Similar to the CdS/Cu(In,Ga)Se_2 system, we find an essentially flat (small-spike) conduction band alignment (here: a conduction band offset of (0.09 ± 0.20) eV), allowing for largely unimpeded electron transfer and forming a likely basis for the success of high-efficiency Zn(O,S)-based chalcopyrite devices. Furthermore, we find evidence for multiple bonding environments of Zn and O in the Zn(O,S) film, including ZnO, ZnS, $Zn(OH)_2$, and possibly ZnSe. Copyright © 2016 John Wiley & Sons, Ltd.

KEYWORDS

chalcopyrite thin-film solar cell; band alignment; alternative buffer layers; Zn(O,S); X-ray spectroscopy; inverse photoemission

***Correspondence**

Michelle Mezher and Clemens Heske, Department of Chemistry and Biochemistry, University of Nevada, Las Vegas (UNLV), 4505 S. Maryland Pkwy Box 454003, Las Vegas, Nevada 89154, USA. mezherm@unlv.nevada.edu, heske@unlv.nevada.edu
E-mail: mezherm@unlv.nevada.edu

Received 24 September 2015; Revised 20 December 2015; Accepted 1 February 2016

1. INTRODUCTION

Cu(In,Ga)Se_2 (CIGSe) thin-film photovoltaic devices have achieved a record efficiency of 22.3% on a laboratory scale [1]. Traditionally, high-efficiency devices contain a CdS buffer layer between CIGSe absorber and transparent front electrode [2]. In contrast, the recent breakthrough was achieved with an alternative Cd-free buffer layer [Zn(O,S)], and other groups have also reported high conversion efficiencies for the Zn(O,S)/CIGSe system [3–6]. Such buffers are desirable as they offer higher transparency and thus the possibility of increasing the current collection in the shorter wavelength region.

A characteristic of record CdS/CIGSe devices is the presence of a flat conduction band alignment at the buffer/absorber interface, both for CdS/$CuInSe_2$ and CdS/Cu(In,Ga)$(S,Se)_2$ [12–14]. In contrast, the less efficient CdS/Cu(In,Ga)S_2 system has been shown to exhibit a cliff-like conduction band offset (CBO) [15]. It is thus important to understand the band alignment at the Zn(O,S)/CIGSe interface by *direct* and independent analysis of the valence *and* conduction band energies without the detrimental effects of sputter depth-profiling, and to compare its commonalities and differences with respect to the CdS-containing CIG(S)Se thin-film photovoltaic systems.

When using Zn(O,S) as a buffer material, it should be noted that ZnS and ZnO have large optical band gaps, 3.54 eV [16] and 3.3 eV [17], respectively, whereas the band gap of the Zn(O,S) alloy can show a strong bowing effect as the O:S ratio varies [18,19], with a minimum at 2.6 eV for a S/(S + O) ratio of 45% [20]. Nevertheless, even at this minimum, Zn(O,S) still exhibits an optical band gap that is approximately 0.2 eV larger than that of CdS (2.4 eV [21]), promising a higher transparency.

To thus gain insights into the electronic level alignment when utilizing Zn(O,S) buffers, it is pertinent to perform a detailed experimental study; here, we present the first non-destructive analysis of the interface using X-ray (XPS) and ultraviolet (UPS) photoelectron spectroscopy as well as inverse photoemission spectroscopy (IPES), investigating samples with varying buffer layer thickness.

2. EXPERIMENTAL

A Zn(O,S)/CIGSe sample series was deposited at National Renewable Energy Laboratory, consisting of a CIGSe "bare" absorber and two Zn(O,S)/CIGSe interface samples of varying Zn(O,S) thickness. The absorbers were deposited onto a Mo-coated soda lime glass substrate using the standard three-stage process and a bulk Ga/(Ga + In) ratio of 0.3 [22]. Our surface-sensitive XPS studies find a Ga/(Ga + In) ratio of 0.33 and 0.32 (±0.10) for the CIGSe and thinnest buffer layer sample, respectively. The Zn(O,S) films were grown by chemical bath deposition (CBD) utilizing zinc sulfate, thiourea, ammonium hydroxide, and dimethyl sulfoxide [23]. Auger depth profiling studies at National Renewable Energy Laboratory showed that the CBD process yielded Zn(O,S) films with a composition of ~25 at% S and ~20 at % O (S/(S + O) ~ 0.56). The CBD time was varied to control the thickness of the Zn(O,S) layer on the absorber—the "thick" Zn(O,S)/CIGSe sample was deposited by the standard 22.5-min CBD process, whereas the "thin" Zn(O,S)/CIGSe sample was deposited by an abbreviated 5 minute CBD. Completed twin devices demonstrated an average efficiency of 17.7% (with a maximum of 17.8%). According to our XPS analysis, the thick layer is clearly a "closed" layer (M. Mezher et al., to be published).

XPS, UPS, and IPES were performed at UNLV to investigate all three samples. XPS measurements were taken using Mg K_α and Al K_α radiation, and He I and II irradiation were used for the UPS measurements. In this paper, only the results obtained with Mg K_α and He I radiation are shown (while the other results nevertheless contributed to the overall interpretation). XPS and UPS measurements were taken with a SPECS PHOIBOS 150 MCD electron analyzer, calibrated using core-level and Auger peaks of clean Ag, Cu, and Au foils (for XPS) [24], and the Fermi energy of the Au foil (for UPS and IPES). All samples were treated with a low-energy (50 eV) Ar^+ ion treatment at a low incidence angle. This has been shown [12,25] to be very effective in removing C and O contaminants from chalcopyrite, CdS, and ZnO surfaces without creating metallic phases commonly found when sputter-cleaning or depth-profiling such surfaces with higher ion energies. The CIGSe absorber was treated for a total of 120 min, and both Zn(O,S)/CIGSe samples were treated for 20 min each to remove (a portion of) the surface adsorbates while minimizing any potential beam damage (note that intense X-ray and electron flood gun irradiation has been shown to induce changes in the zinc hydroxide/zinc oxide ratio of hydroxide-rich films [26,27]). All peaks were analyzed by fitting the different spectral intensities with Voigt functions (with coupled Lorentzian and Gaussian widths) and a linear background using the Fityk peak-fitting program [28]. A commercial low-energy electron gun (Staib) and a home-built Dose-type detector with a SrF_2 window and Ar:I_2 filling [29] were used for IPES experiments. The valence band maximum (VBM) and conduction band minimum (CBM) were determined by linear extrapolation of the leading edge in the valence band (UPS) and conduction band (IPES) spectra [30]. The base pressure in the chamber was $<5 \times 10^{-10}$ mbar.

3. RESULTS AND DISCUSSION

Figure 1 presents Mg K_α XPS spectra of the O 1 s region of the thick and thin Zn(O,S)/CIGSe samples. The shape and broadness of the O 1 s peak in both samples indicate the presence of multiple chemical species. Indeed, a fit analysis shows that a single Voigt peak does not give a satisfactory description, indicating that at least two species are present. Conversely, we find that the quality of the fit achieved with two Voigt functions for each O 1 s region (with a linear background and identical Gaussian and Lorentzian widths for all the species) is already very high and that a third component does not lead to a significant further improvement. Consequently, the residuals shown below each spectrum show a statistical distribution without any evidence for additional peaks.

Comparing the binding energies with values from literature, the two components for both samples can be assigned to ZnO and $Zn(OH)_2$ [31,32]. Because the Zn (O,S) is deposited onto the CIGSe via a wet-chemical deposition route, Zn-OH bonds are not unexpected [5], suggesting that the dehydrogenation of the Zn(O,S) layer is incomplete for both the thin and thick Zn(O,S)/CIGSe samples [18,33]. The possibility of a sulfate species was also taken into account because the O 1 s peak location of a sulfate species and a hydroxide species are similar. However, none of our sulfur XPS spectra show any evidence for sulfates. Overall, our XPS, X-ray excited Auger electron spectroscopy, and X-ray emission spectroscopy results suggest the presence of up to four different Zn species (associated with Zn-containing bonds similar to those in ZnO, ZnS, $Zn(OH)_2$, and ZnSe) (M. Mezher et al., to be published).

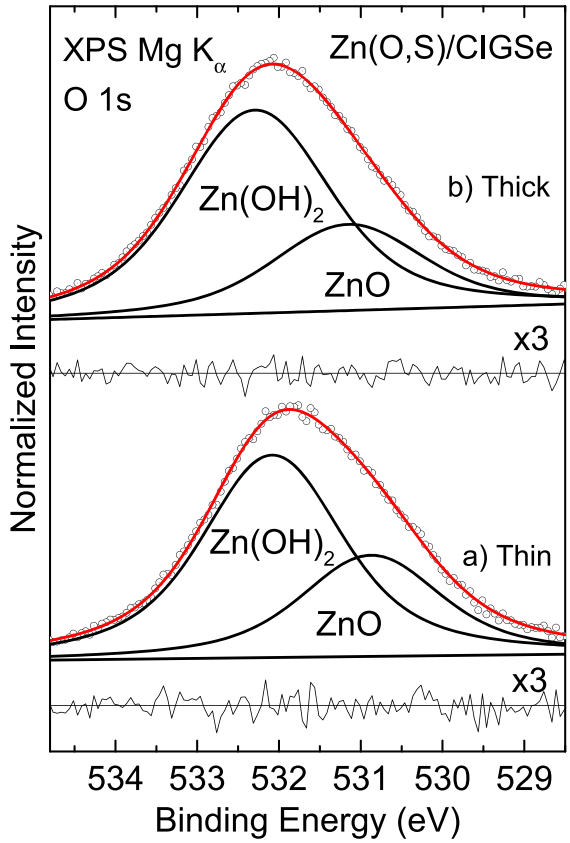

Figure 1. XPS detail spectra of the O 1 s peak and fit (components in black, sum in red) of (a) the thin (5 min) and (b) the thick (22.5 min) Zn(O,S)/CIGSe samples. The magnified residual of each fit is also shown.

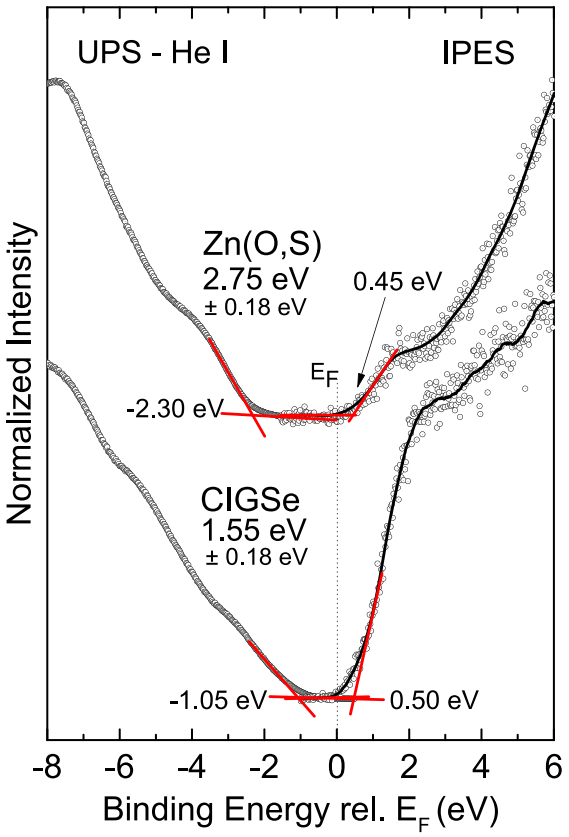

Figure 2. He I UPS (left) and IPES (right) spectra of the bare CIGSe absorber (bottom) and the thick Zn(O,S)/CIGSe sample (top). VBM and CBM values determined by linear extrapolations of the leading edges (red lines) are shown, together with the resulting electronic surface band gaps. Error bars are ±0.10 and ±0.15 eV for the VBM and CBM determination, respectively. A Savitzky–Golay-smoothed line is shown for the IPES spectra as a guide to the eye.

UPS and IPES spectra to analyze the valence (VB) and conduction band (CB), respectively, of the bare CIGSe absorber and the thick (22.5 min) Zn(O,S) CBD buffer layer are shown in Figure 2. The VBM and CBM for the bare CIGSe absorber are found at -1.05 (±0.10) below and 0.50 (±0.15) eV above the Fermi energy, respectively. The thus derived electronic surface band gap of 1.55 (±0.18) eV agrees well with previously measured CIGSe surface band gaps of high efficiency absorbers with Cu-poor surfaces [12–14,34–36]. The VBM and CBM of the Zn(O,S) layer are found at -2.30 (±0.10) eV and 0.45 (±0.15) eV, respectively, deriving an electronic surface band gap of 2.75 (±0.18) eV. Note that the optical (bulk) band gap of a pure Zn(O,S) alloy with a S/(S + O) ratio of ~56% is expected to be ~2.6 (±0.10) eV [20]. A larger Zn (O,S) surface band gap in our case might be because of various reasons, including the presence of Zn–OH bonds (as shown by the O 1 s spectra) and the previously mentioned presence of multiple Zn-containing species [33].

To derive a complete description of the band alignment at the interface, additional information is needed to take into account how the band bending at the absorber surface changes during the formation of the interface, as well as whether/how a band bending evolves in the buffer layer (as a function of thickness). For this purpose, the thin Zn (O,S)/CIGSe sample serves as an intermediate step in the interface formation (note that it is not possible to derive electronic structure information from an interface by sputter depth-profiling through the top layer because of the induced structural and chemical defects and compositional changes associated with preferential sputtering). Deriving the band bending changes is performed by comparing the core-level peak positions of the CIGSe absorber (Se, In, Cu) to those of the thin Zn(O,S)/CIGSe sample, as listed in Table I (top). The observed shifts lie between 0.03 eV and 0.10 eV and indicate a very small *upward* shift [0.06 eV] of the absorber surface band edges as the interface starts to form. In other words: the (expected) downward band bending at the absorber surface is slightly reduced by the interface formation. This needs to be compared with the CdS/CIG(S)Se system, where we either find a negligible impact on the band edge positions [12–14] or a

Table I. Core level peak positions of the bare absorber, the thin (5 min) Zn(O,S)/CIGSe sample, and the thick (22.5 min) Zn(O,S)/CIGSe sample, as well as their relative shifts.

Core level	CIGSe BE (eV)	Thin 5 min Zn(O,S) BE (eV)	Shift
Se 3d	54.33	54.30	0.03
In $3d_{5/2}$	444.78	444.68	0.10
Cu $2p_{3/2}$	932.56	932.52	0.04
Core level	**Thin 5 min Zn(O,S) BE (eV)**	**Thick 22.5 min Zn(O,S) BE (eV)**	**Shift**
S $2p_{3/2}$	161.91	162.12	0.21
O 1 s ($Zn(OH)_2$)	532.06	532.25	0.19
O 1 s (ZnO)	530.89	531.08	0.19
Zn $2p_{3/2}$	1022.33	1022.41	0.08

small additional downward shift (unpublished). The here-observed (small) upward shift could have several origins, including a small change in the CIGSe surface dipole upon becoming an interface dipole to the Zn(O,S) layer, and a possible charge transfer across the interface to influence the space-charge region. The latter interpretation would require that the Fermi level at the interface is not pinned.

To investigate whether/how band bending evolves in the buffer layer as a function of thickness, the core-level binding energy (BE) differences between the thin and thick Zn(O,S) samples (Zn, O, and S core levels) are compared, as listed in Table I (bottom). As the buffer layer thickness increases, the Zn, O, and S core-level peaks from the thin Zn(O,S)/CIGSe sample also shift toward lower BE. For a quantitative analysis, we need to take into account that the buffer layer consists of multiple chemical species, as discussed in the preceding texts. For oxygen, we thus analyze both components (i.e., the ZnO and $Zn(OH)_2$ species) separately in order to avoid spurious peak shifts because of a variation in $ZnO/Zn(OH)_2$ ratio. For sulfur, we expect one dominant species (ZnS), and thus, the S $2p_{3/2}$ BE is taken "as derived". For Zn, finally, we argue that there are too many different species overlapping within the Zn $2p_{3/2}$ peak, and thus, it is not possible to separate band bending effects from variations in relative abundance of the different species. We therefore list the BE values in Table I, but do not use them for the band alignment determination (hence shaded gray in Table. I). Overall, we derive a shift of 0.20 eV for the buffer layer core levels. Note that the S and O core levels all shift in unison, suggesting that these shifts are because of band bending in the buffer layer, rather than to chemical shifts because of an altered S/(S + O) or OH/(O + OH) ratio in the buffer layer itself. This interpretation is corroborated by a quantitative analysis of the OH/(O + OH) ratio, which derives values for the 5 and 22.5 min Zn(O,S) samples (M. Mezher et al., to be published) that are equal within the error bars of such a determination.

The full band alignment of the Zn(O,S)/CIGSe interface, including the band bending correction, is depicted in Figure 3. A small conduction band offset (CBO = 0.09 ± 0.20 eV) is found, indicating that the conduction band alignment at the Zn(O,S)/CIGSe interface is essentially flat

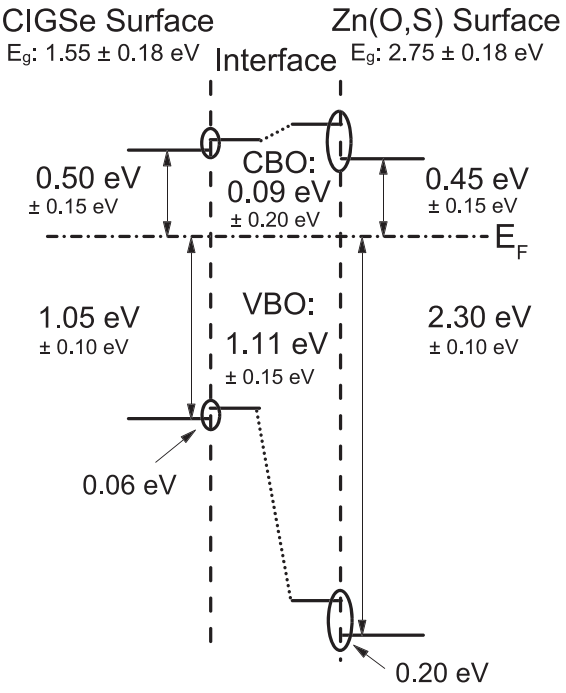

Figure 3. Band alignment scheme of the Zn(O,S)/CIGSe interface. The band edge positions at the CIGSe and Zn(O,S) surfaces are shown on the left and right, respectively. In the center, the band alignment at the interface is shown, taking interface-induced band bending changes at the absorber surfaces and band bending in the buffer layer into account (as indicated by the ovals).

(small spike), as in [12–14,27]. Likewise, a considerable valence band offset (VBO = 1.15 ± 0.15 eV) is formed, creating a hole barrier and decreasing interfacial recombination. Note that the error bars were determined as a best-faith estimate of the Gaussian distribution around the derived value (they should not be misinterpreted as a "box of equal probability").

As mentioned in the introduction, we have consistently found flat conduction alignments in optimized CIG(S)Se-based devices [12–14], with the exception of CdS/Cu(In, Ga)S_2, for which a cliff was found [15]. Given the fact that

the O/S ratio of the Zn(O,S) layer gives an additional optimization parameter for this alternative buffer layer, it is not necessarily to be expected that a flat conduction band alignment is found. In particular, modeling studies have suggested that buffer/absorber interfaces are far less sensitive towards spikes than towards cliff arrangements [37–39]. Nevertheless, empirical optimization time-and-again leads to electronic level alignments that are very close to "flat", suggesting that such an optimized level alignment should be considered one of the primary design criteria for constructing deliberately tailored thin film photovoltaic devices.

4. CONCLUSION

The electronic structure of the Zn(O,S)/CIGSe interface was analyzed using X-ray, UV, and inverse photoemission. We find evidence for multiple chemical environments of oxygen in the Zn(O,S) buffer layer, best described by ZnO and Zn$(OH)_2$ components. Detailed analysis of the bare CIGSe and thick Zn(O,S)/CIGSe samples, together with an optimally chosen thin Zn(O,S) intermediate sample to monitor variations of band bending because of interface formation and increasing buffer layer thickness, allowed for a comprehensive and all-experimental depiction of the electronic level alignment at the interface. We find an essentially flat conduction band alignment (small spike) and a significant valence band offset (i.e., a hole barrier). Such a structure is expected to allow for unobstructed electron transport across this interface, beneficial for high-efficiency thin-film solar cells.

ACKNOWLEDGEMENTS

We gratefully acknowledge funding from the Department of Energy (DOE) through the F-PACE Partnership (subcontract No. ZEJ-2-22082-0.1). M. Bär additionally acknowledges funding by the Impuls- und Vernetzungsfonds of the Helmholtz Association (VH-NG-423).

REFERENCES

1. "Solar Frontier Achieves World Record Thin-Film Solar Cell Efficiency: 22.3%" [Online]. Available: http://www.solar-frontier.com/eng/news/2015/C051171.html. Accessed: January 15, 2016.
2. Jackson P, Hariskos D, Wuerz R, Kiowski O, Bauer A, Friedlmeier TM, Powalla M. Properties of Cu(In,Ga)Se_2 solar cells with new record efficiencies up to 21.7%. *Physica Status Solidi Rapid Research Letters* 2014; **9**(1): 28–31. DOI:10.1002/pssr.201409520.
3. "ZSW raises efficiency of cadmium-free CIGS solar cells to record 21%." [Online]. Available:http://www.semiconductortoday.com/news_items/2015/feb/zsw_250215.shtml. Accessed: May 15, 2015.
4. Contreras MA, Nakada T, Hongo M, Pudov OA, Sites JR. ZnO/ZnS(O,OH)/Cu(In,Ga)Se_2/Mo solar cell with 18.6% efficiency. *Proceedings of 3rd World Conference on Photovoltaic Energy Conversion* 2003; 1: 570-573.
5. Hariskos D, Menner R, Jackson P, Paetel S, Witte W, Wischmann W, Powalla M, Bürkert L, Kolb T, Oertel M, Dimmler B, Fuchs B. New reaction kinetics for a high-rate chemical bath deposition of the Zn(S,O) buffer layer for Cu(In,Ga)Se_2-based solar cells. *Progress in Photovoltaics: Research and Applications* 2012; **20**(5): 534–542. DOI:10.1002/pip.1244.
6. Klenk R, Steigert A, Rissom T, Greiner D, Kaufmann CA, Unold T, Lux-Steiner MC. Junction formation by Zn(O,S) sputtering yields CIGSe-based cells with efficiencies exceeding 18%. *Progress in Photovoltaics: Research and Applications* 2014; **22**(2): 161–165. DOI:10.1002/pip.2445.
7. Bär M, Ennaoui A, Klaer J, Sáez-Araoz R, Kropp T, Weinhardt L, Heske C, Schock HW, Lux-Steiner MC. The electronic structure of the [Zn(S,O)/ZnS]/$CuInS_2$ heterointerface – impact of post-annealing. *Chemical Physics Letters* 2006; **433**(1-3): 71–74. DOI:10.1016/j.cplett.2006.11.022.
8. Grimm A, Just J, Kieven D, Lauermann I, Palm J, Neisser A, Rissom T, Klenk R. Sputtered Zn(O,S) for junction formation in chalcopyrite-based thin film solar cells. *Physical Status Solidi RRL* 2010; **4**(5-6): 109–111. DOI:10.1002/p22r.201004083.
9. Kieven D, Grimm A, Lauermann I, Lux-Steiner MC, Palm J, Niesen T, Klenk R. Band alignment at the sputtered ZnS_xO_{1-x}/Cu(In,Ga)$(Se,S)_2$ heterojunctions. *Physical Status Solidi RRL* 2012; **6**(7): 294–296. DOI:10.1002/pssr.201206195.
10. Pankow JW, Steirer KW, Mansfield LM, Garris RL, Ramanathan K, Teeter GR. Photovoltaic Specialist Conference (PVSC), 2014 IEEE 40th 2014; 1670-1673. DOI: 10.1109/PVSC.2014.6925240.
11. Terada N, Morita H, Chochi K, Yoshimoto S, Mitsunaga M, Ishizuka S, Shibata H, Yamada A, Matsubara K, Niki S. Characterization of electronic structure of oxysulfide buffers and band alignment at buffer/absorber interfaces in Cu(In,Ga)Se_2-based solar cells. *Japanese Journal of Applied Physics* 2014; **53**: 05W09-1–05FW09-5. DOI:10.7567/JJAP.53.05FW09.
12. Morkel M, Weinhardt L, Lohmüller B, Heske C, Umbach E, Riedl W, Zweigart S, Karg F. Flat conduction-band alignment at the CdS/$CuInSe_2$ thin-film solar-cell heterojunction. *Applied Physics Letters* 2001; **79**(27): 4482–4484. DOI:10.1063/1.1428408.
13. Weinhardt L, Morkel M, Gleim T, Zweigart S, Niesen T.P, Karg F, Heske C, Umbach E. Band alignment at

the CdS/CuIn(S,Se)$_2$ heterojunction in thin film solar cells. *Proceedings 17th European Photovoltaic Solar Energy Conference* 2001; 1261.

14. Weinhardt L, Fuchs O, Groβ D, Storch G, Dhere NG, Kadam AA, Kulkarni SS, Visbeck S, Niesen TP, Karg F, Heske C, Umbach E. Comparison of band alignments at various CdS/Cu(In,Ga)(S,Se)$_2$ interfaces in thin film solar cells. *Conference Record of the 2006 IEEE 4th World Conference on Photovoltaic Energy Conversion* 2006; 1: 412–415.
15. Weinhardt L, Fuchs O, Groß D, Storch G, Umbach E, Dhere NG, Kadam AA, Kulkarni SS, Heske C. Band alignment at the CdS Cu(In,Ga)S_2 interface in thin-film solar cells. *Applied Physics Letters* 2005; **86**(6): 062109–062109-3. DOI:10.1063/1.1861958.
16. Hervé P, Vandamme LKJ. General relation between refractive index and energy gap in semiconductors. *Infrared Physics Technology* 1994; **35**(4): 609–615. DOI:10.1016/1350-4495(94)90026-4.
17. Srikant V, Clarke DR. On the optical band gap of zinc oxide. *Journal of Applied Physics* 1998; **83**(10): 5447–5451. DOI:10.1063/1.367375.
18. Eicke A, Ciba T, Hariskos D, Menner R, Tschamber C, Witte W. Depth profiling with SNMS and SIMS of Zn(O,S) buffer layers for Cu(In,Ga)Se_2 thin-film solar cells. *Surface and Interface Analysis* 2013; **45**: 1811–1820. DOI:10.1002/sia.5325.
19. Platzer-Björkman C, Törndahl T, Abou-Ras D, Malmström J, Kessler J, Stolt L. Zn(O,S) buffer layers by atomic layer deposition in Cu(In,Ga)Se_2 based thin film solar cells: band alignment and sulfur gradient. *Journal of Applied Physics* 2006; **100**: 044506. DOI:10.1063/1.2222067.
20. Meyer BK, Polity A, Farangis B, He Y, Hasselkamp D, Krämer T, Wang C. Structural properties and bandgap bowing of $ZnO_{1-x}S_x$ thin films deposited by reactive sputtering. *Applied Physics Letters* 2004; **85**(21): 4929–4931. DOI:10.1063/1.1825053.
21. De Melo O, Hernández L, Zelaya-Angel O, Lozada-Morales R, Becerril M, Vasco E. Low resistivity cubic phase CdS films by chemical bath deposition technique. *Applied Physics Letters* 1994; **65**(10): 1278–1280. DOI:10.1063/1.112094.
22. Contreras MA, Egaas B, Ramanathan K, Hiltner J, Swartzlander A, Hasoon F, Noufi R. Progress toward 20% efficiency in Cu(In,Ga)Se_2 polycrystalline thin-film solar cells. *Progress in Photovoltaics: Research and Applications* 1999; **7** (4): 311–316. DOI:10.1002/(SICI)1099-159X(199907/08)7:4<311::AID-PIP274>3.0.CO;2-G.
23. Ramanathan K, Mann J, Glynn S, Christensen S, Pankow J, Li J, Scharf J, Mansfield L, Contreras M, Noufi R. A comparative study of Zn(O,S) buffer layers and CIGS solar cells fabricated by CBD, ALD, and sputtering. *2012 38th IEEE Photovoltaic Specialists Conference (PVSC)* 2012; 001677-001681. DOI: 10.1109/PVSC.2012.6317918.
24. Briggs D, Seah MP (Eds). *Practical Surface Analysis, 2nd Edition, vol I, Auger and X-ray Photoelectron Spectroscopy*Appendix 1: Spectrometeter energy scale calibration. Appendix 1 edited by Seah MP, Smith GC. John Wiley: New York, 1990.
25. Weinhardt L, Heske C, Umbach E, Niesen TP, Visbeck S, Karg F. Band alignment at the i-ZnO/CdS interface in Cu(In,Ga)(S,Se)$_2$ thin-film solar cells. *Applied Physics Letters* 2004; **84**(16): 3175–3177. DOI:10.1063/1.1704877.
26. Duchoslav J, Steinberger R, Arndt M, Stifter D. XPS study of zinc hydroxide as a potential corrosion product of zinc: rapid X-ray induced conversion into zinc oxide. *Corrosion Science* 2014; **82**: 356–361. DOI:10.1016/j.corsci.2014.01.037.
27. Reichardt J, Bär M, Grimm A, Kötschau I, Lauermann I, Sokoll S, Lux-Steiner MC, Fischer C-H, Heske C, Weinhardt L, Fuchs O, Jung C, Gudat W, Karg F. Inducing and monitoring photoelectrochemical reactions at surfaces and buried interfaces in Cu(In,Ga)(S,Se)$_2$ thin film solar cells. *Applied Physics Letters* 2005; **86**: 172102. DOI:10.1063/1.1906309.
28. Wojdyr M. Fityk: a general-purpose peak fitting program. *Journal of Applied Crystallography* 2010; **43** (5-1): 1126–1128. DOI:10.1107/S0021889810030499.
29. Denninger G, Dose V, Scheidt H. A VUV isochromat spectrometer for surface analysis. *Applied Physics* 1979; **18**(4): 375–380. DOI:10.1007/BF00899691.
30. Gleim T, Heske C, Umbach E, Schumacher C, Gundel S, Faschinger W, Fleszar A, Ammon C, Probst M, Steinrück HP. Formation of the ZnSe/(Te/)GaAs(1 0 0) heterojunction. *Surface Science* 2003; **531**(1): 77–85. DOI:10.1016/S0039-6028(03)00439-4.
31. Moulder JF, Stickle WF, Sobol PE, Bomben KD, Chastain J (Eds). *Handbook of X-Ray Photoelectron Spectroscopy*. Perkin-Elmer, Eden Prairie, 1992.
32. Deroubaix G, Marcus P. X-ray photoelectron spectroscopy analysis of copper and zinc oxides and sulphides. *Surface and Interface Analysis* 1992; **18**: 39–46. DOI:10.1002/sia.740180107.
33. Weinhardt L, Bär M, Muffler HJ, Fischer CH, Lux-Steiner MC, Niesen TP, Karg F, Gleim T, Heske C, Umbach E. Impact of Cd^{2+}-treatment on the band alignment at the ILGAR-ZnO/CuIn(S,Se)$_2$ heterojunction. *Thin Solid Films* 2003; **431-432**: 272–276. DOI:10.1016/S0040-6090(03)00270-0.
34. Bär M, Repins I, Contreras MA, Weinhardt L, Noufi R, Heske C. Chemical and electronic surface structure

of 20%-efficient Cu(In,Ga)Se_2 thin film solar cell absorbers. *Applied Physics Letters* 2009; **95**(5): 052106–052106-3. DOI:10.1063/1.3194153.

35. Bär M, Nishiwaki S, Weinhardt L, Pookpanratana S, Fuchs O, Blum M, Yang W, Denlinger JD, Shafarman WN, Heske C. Depth-resolved band gap in Cu(In,Ga)$(S,Se)_2$ thin films. *Applied Physics Letters* 2008; **93** (24): 244103–244103-3. DOI:10.1063/1.3046780.
36. Horsley K, Pookpanratana S, Krause S, Hofmann T, Blum M, Weinhardt L, Bär M, George K, Van Duren J, Jackrel D, Heske C. Electronic and chemical properties of non-vacuum deposited chalcopyrite solar cells. *Photovoltaic Specialists Conference (PVSC), 2011 37th IEEE* 2011; 000374-000378. DOI: 10.1109/PVSC.2011.6185972.
37. Niemegeers A, Burgelman M, De Vos A. On the CdS/$CuInSe_2$ conduction band discontinuity. *Applied Physics Letters* 1995; **67**: 843–845. DOI:10.1063/1.115523.
38. Xiaoxiang L, Sites JR. Calculated effect of conduction-band offset on $CuInSe_2$ solar-cell performance. *AIP Conference Proceedings* 1996; **353**: 444–452. DOI:10.1063/1.49373.
39. Wei S-H, Zunger A. Band offsets at the CdS/$CuInSe_2$ heterojunction. *Applied Physics Letters* 1993; **63**: 2549–2551. DOI:10.1063/1.110429.